Dynamic PET Reconstruction Utilizing a Spatiotemporal 4D De-noising Kernel

Ju-Chieh (Kevin) Cheng, *Member, IEEE*, Connor Bevington, *Student Member, IEEE*, Arman Rahmim, *Member, IEEE*, Ivan Klyuzhin, *Member, IEEE*, Julian Matthews, Ronald Boellaard, and Vesna Sossi, *Member, IEEE*

***Abstract*: We propose novel 4D de-noised image reconstruction frame works, followed by extensive validation using 4D simulations, experimental phantom as well as clinical patient data. Previously, it was demonstrated that our 3D de-noised reconstruction, which applies the HighlY constrained backPRojection (HYPR) de-noising operator After each Update of OSEM (HYPR-AU-OSEM), can achieve noise reduction and improve the reproducibility in contrast recovery without degrading accuracy in terms of resolution and contrast for single frame reconstruction. Moreover, the method does not require any prior information and is not computationally intensive. In this work, we propose the 4D extension of HYPR-AU-OSEM (i.e. HYPR4D-AU-OSEM) for dynamic imaging. Further, we incorporate the proposed 4D de-noising operator within the recently proposed kernelized reconstruction frame work (i.e. HYPR4D-K-OSEM) inspired by machine learning. In short, the proposed methods make use of the spatiotemporal high frequency features extracted from the 4D composite, generated directly within the reconstruction, to preserve the 4D resolution and constrain the noise increment in both spatial and temporal domains. Results from the simulations, experimental phantom, and patient data showed that the proposed methods outperformed the standard OSEM with post filter in terms of 4D resolution, contrast recovery coefficient vs noise trade-off, and accuracy in time-activity-curves (TAC) and binding potential (BP_{ND}) values. In particular, the root mean squared error in regional BP_{ND} values was reduced from ~8% to ~3% using the proposed methods. Compared to the conventional 3D composite, the 4D composite achieved 50% lower mean absolute error in TACs. Comparable results were obtained between AU and kernel methods. In summary, the improvement in 4D resolution and noise reduction obtained from the proposed methods can produce more robust and accurate image features without any prior information, as compared to the conventional methods.**

Manuscript received December 13, 2018. This work was supported by the Natural Sciences and Engineering Research Council of Canada (NSERC) grant.

J.-C. Cheng is with the Pacific Parkinson's Research Centre and Department of Physics and Astronomy, The University of British Columbia, Vancouver, B.C. Canada (email: chengj@mail.ubc.ca). C. Bevington, A. Rahmim, and V. Sossi are with the Department of Physics and Astronomy, The University of British Columbia, Vancouver, B.C. Canada (email: bevington@phas.ubc.ca, arman.rahmim@ubc.ca, and vesna@phas.ubc.ca). I. Klyuzhin is with the Department of Medicine, Division of Neurology, University of British Columbia, Vancouver, B.C., Canada (email: ivansk@physics.ubc.ca). J. Matthews is with the Division of Informatics, Imaging, and Data Sciences, the University of Manchester, MAHSC, Wolfson Molecular Imaging Centre, Manchester, The United Kingdom (e-mail: Julian.Matthews@manchester.ac.uk). R. Boellaard is with the Department of Radiology and Nuclear Medicine, VU University Medical Center, Amsterdam and the Department of Nuclear Medicine and Molecular Imaging, University Medical Center Groningen, The Netherlands (e-mail: r.boellaard@vumc.nl).

I. Introduction

Reconstructed PET images are typically noisy, especially in dynamic imaging where the acquired data are divided into several short frames. As a result, the signal-to-noise ratio (SNR) in these short frame images is very poor since the SNR is directly proportional to the frame duration. Recently, a novel reconstruction method which incorporates HighlY constrained back-PRojection (HYPR) de-noising directly within the widely used OSEM algorithm (i.e. HYPR-AU-OSEM) [1] has been proposed. Our previous work demonstrated that HYPR-AU-OSEM can achieve noise reduction and improve the reproducibility in contrast recovery without degrading accuracy in terms of resolution and contrast for single frame reconstruction. Further, the method does not require any prior information and is not computationally intensive. In this work, we will present (i) the 4D extension of our de-noised reconstruction for dynamic imaging, and (ii) incorporation of our 4D de-noising operator within the recently proposed kernelized reconstruction [2]. The proposed methods were compared with standard methods using simulation, experimental phantom, and clinical human data.

II. Methods

4D Composite and HYPR4D-AU-OSEM

In dynamic imaging, the composite image, which provides guidance to improve the SNR either in post processing de-noising or directly within the reconstruction task, is typically generated by summing the temporal data [2][3]. However, this approach is highly sensitive to drastic change in tracer distribution since the composite would introduce bias to the target image when the contrast in the composite is very different from that in the target [4]; e.g. the spatiotemporal features or shapes of the time-activity-curves (TAC) may not be well preserved. To minimize the bias, the composite images were typically generated by summing data from a limited number of nearby frames; consequently, the noise reduction is usually not effective since the composite images are still quite noisy. Instead of summing temporal data to generate 3D composite, in this work we propose a spatiotemporal 4D composite based on the following observation.

In our previous de-noised reconstruction frame work, the composite was generated directly within the single frame reconstruction and updated for each OSEM iteration as the sum of the preceding subset images from the previous iteration [1]. When reconstructing 4D data set (i.e. multiple frame images) using this approach, one can generate a frame-independent composite for each time point, and this dynamic

series of composites forms the 4D composite (i.e. there is a one-to-one dynamic voxel matching between the 4D image estimate and the 4D composite) which enables the de-noising operation to be applicable in both spatial and temporal domains. Based on this observation, the proposed HYPR4D de-noising operator (H_{4D}^m) is defined in Eq.(1) where m and s correspond to the OSEM iteration and subset indices, respectively; C_{4D} and I_{4D} represent the composite and the target image, respectively, and F_{4D} is the 4D Gaussian filter in this case. Here the contrast in the composite is ensured to be close to that in the target as the 4D composite is updated every iteration.

$$H_{4D}^m(I_{4D}^{m,s}) = H_{C_{4D}^m;F_{4D}}(I_{4D}^{m,s}) = C_{4D}^m \cdot \frac{F_{4D} * I_{4D}^{m,s}}{F_{4D} * C_{4D}^m}, \text{and}$$
$$C_{4D}^m = \sum_s I_{4D}^{m-1,s} \quad (1)$$

The HYPR4D-AU-OSEM is thus given by:

$$\lambda_{4D}^{m,s} = H_{4D}^m\left[\frac{\lambda_{4D}^{m,s-1}}{P_s^T 1} \cdot \left(P_s^T \frac{y_{4D}^s}{P_s \lambda_{4D}^{m,s-1} + b_{4D}^s}\right)\right] \quad (2)$$

Here all dynamic images are updated at once as the 4D image estimate (λ_{4D}). In summary, the proposed method makes use of the spatiotemporal high frequency features extracted from the 4D composite, generated directly within the reconstruction, to preserve the 4D resolution and constrain the noise in both spatial and temporal domains.

HYPR4D-K-OSEM

Typically, kernelized reconstruction methods [2] reparameterize the EM algorithm into an alternative set of spatial basis functions (i.e. kernel matrix K) and kernel coefficients (α). In this work, the proposed HYPR4D de-noising operator forms a set of spatiotemporally variant convolutional basis functions within the kernel matrix which constrains the noise increment in both spatial and temporal domains while effectively updating the 4D contrast. The proposed 4D de-noised kernel OSEM (HYPR4D-K-OSEM) is defined as:

$$\alpha_{4D}^{m,s} = \frac{\alpha_{4D}^{m,s-1}}{(K_{H4D}^m)^T P_s^T 1} \cdot \left((K_{H4D}^m)^T P_s^T \frac{y_{4D}^s}{P_s K_{H4D}^m \alpha_{4D}^{m,s-1} + b_{4D}^s}\right)$$
$$\lambda_{4D}^{m,s} = K_{H4D}^m \alpha_{4D}^{m,s} \quad (3)$$

where the HYPR4D kernel matrix (K_{H4D}^m) is given by:

$$K_{H4D}^m = diag[h^m]F_{4D}, \text{where} \quad h^m = \frac{C_{4D}^m}{F_{4D} * C_{4D}^m},$$
$$C_{4D}^m = \sum_s K_{H4D}^{m-1} \alpha_{4D}^{m-1,s} \quad (4)$$

Here the spatiotemporally variant convolutional kernel matrix is decomposed into the normalized 4D high frequency features (h^m) extracted from the 4D composite and the spatiotemporally invariant 4D Gaussian convolution (F_{4D}). The sparsity of the kernel matrix only depends on the width of the 4D Gaussian since the matrix which contains h^m is diagonal. Similar to the AU method, the proposed kernel matrix is updated along with the 4D composite every iteration. For both AU and kernel methods, one iteration of standard OSEM was used to initialize the composite in the 4D de-noising operator and kernel matrix. After the 2nd iteration, the composite is updated using the de-noised images from the previous iteration thus providing a highly constrained noise increment per update and allowing the 4D high frequency features to be updated in a cleaner fashion as compared to the conventional methods.

Experimental phantom, simulation, and clinical human studies

For the reconstructions of the contrast phantom study acquired on the HRRT [5], up to 12 iterations with 16 subsets were used for all methods. The Gaussian post filter applied to OSEM images had a FWHM of 2mm in all cases. The phantom data were histogrammed using a typical tracer protocol (4x60s, 3x120s, 8x300s, 1x600s) to generate dynamic sinogram data. An artificial temporal pattern was created by not correcting for the radioactive decay and image frame duration (i.e. sharp temporal peaks and dips were formed by the difference in frame duration and the radioactive decay of ^{18}F). The reference was generated from the average of high count OSEM reconstructions and by assuming constant (fully corrected) activity across time (i.e. a horizontal TAC). The uncorrected reference TAC was then created by de-correcting the straight TAC for decay and frame duration. The contrast recovery coefficient (CRC) versus image voxel noise was also evaluated at a low count situation (20 million).

The 4D simulations of dynamic [^{11}C]PiB and [^{11}C]RAC scans similar to that described in [6] were used for evaluations of time-varying tracer distribution. In order to focus on the effect due to noise, eroded regions of interest were used to minimize the partial volume effect/cross-talk contamination. Mean Absolute Error (MAE) in regional activity across all time points was used as the metric when comparing the TACs between reconstruction methods. Regional binding potential (BP_{ND}) values were compared between methods as well. In addition, a dynamic human [^{11}C]Raclopride (RAC) study acquired on the HRRT was included for the validation. TACs and parametric BP_{ND} images were compared between methods.

III. Results and Discussions

Results from the simulations, experimental phantom, and patient data showed that the proposed methods outperformed the standard OSEM with post filter in terms of 4D resolution, CRC vs noise trade-off, and accuracy in TACs and BP_{ND} values (see Figs. 1, 2, and Table 1). In particular, the root mean squared error in regional BP_{ND} values was reduced from ~8% to ~3% using the proposed methods. The 4D composite was also demonstrated to outperform the conventional 3D composite in terms of accuracy in TACs (MAE was reduced from 448 Bq/cc to 235 Bq/cc). Better CRC vs noise trajectories can be achieved by using wider kernel sizes for both HYPR4D-K and HYPR4D-AU methods. A wider kernel

needs to be used in the kernel method to achieve similar CRC vs noise trade-off; however, the kernel method has faster convergence rate in CRC especially in small hot regions as compared to the AU method. In summary, the improvement in 4D resolution and 4D noise reduction obtained from the proposed methods can produce more robust and accurate image features without any prior information, as compared to the conventional methods.

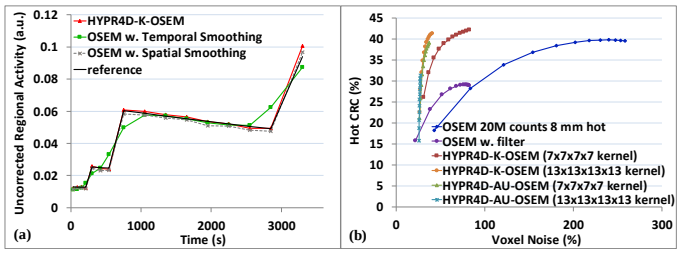

Fig. 1. (a) The uncorrected TAC extracted from various reconstruction methods for the experimental contrast phantom study. The spatial filtering introduced a consistent underestimation in regional activity across time points while the temporal filtering altered the pattern along the TAC (e.g. all sharp peaks and dips were removed). The proposed method, however, preserved both regional activity and temporal pattern (i.e. 4D resolution). The AU method showed nearly identical results as the kernel method (not shown). (b) CRC vs voxel noise comparison at low count level for the 8mm hot insert. Each data point represents an OSEM iteration, and the data were extracted from phantom images reconstructed using standard OSEM with and without post filter, HYPR4D-K-OSEM, and HYPR4D-AU-OSEM with different 4D kernel sizes.

Table 1. MAE comparison from the PiB simulation. The noise-free TAC peaks at ~17000 Bq/cc. OSEM was performed on both noisy and noise-free data using the standard protocol (6 iterations with 16 subsets). The lowest MAE from each de-noised reconstruction is listed below:

Recon. Method	OSEM w. filter	HYPR-K-OSEM w. conventional 3D composite 13x13x13 3D kernel	HYPR4D-K-OSEM w. 7x7x7x7 (13x13x13x13) 4D kernel	HYPR4D-AU-OSEM w. 7x7x7x7 4D kernel	OSEM on noise-free data
MAE (Bq/cc)	**551**	**448**	**319 (235)**	**267**	**174**

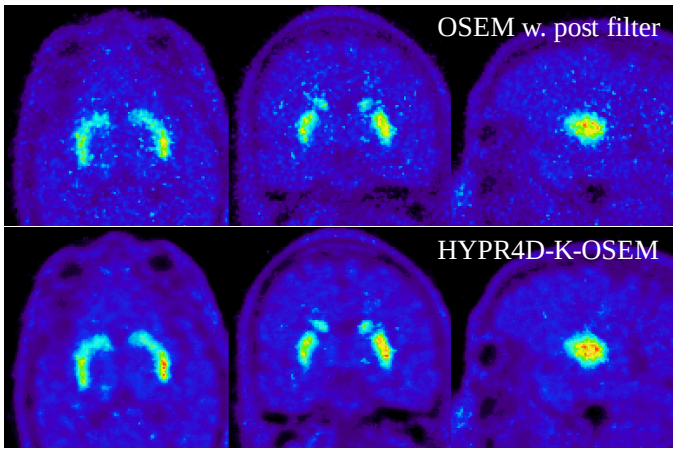

Fig. 2. Parametric BP_{ND} images generated from (top) OSEM with post filter and (bottom) HYPR4D-K-OSEM (same color scale) for the human RAC scan. Better structure boundary definition, higher contrast, less noisy and ~15% higher BP_{ND} values in the target regions can be observed from the HYPR4D-K-OSEM reconstruction, whereas high frequency features contain more noise and/or are buried by the post filter in the filtered OSEM image.

REFERENCES

[1] Cheng et al., Phys. Med. Biol., 62: 6666-6687, 2017.
[2] Wang et al., IEEE Trans. Med. Imag., 34(1): 61-71, 2015.
[3] Christian et al., J. Nucl. Med., 51(7): 1147-1154, 2010.
[4] Floberg et al., Med Phys., 39(6): 3319-3331, 2012.
[5] De Jong et al., Phys. Med. Biol., 52: 1505-1526, 2007.
[6] Lu et al., Phys. Med. Biol., 57: 5035-5055, 2012.